Zhu, Ya; Huan, Siqi; Bai, Long; Ketola, Annika; Shi, Xuetong; Zhang, Xiao; Ketoja, Jukka A.; Rojas, Orlando J.

High Internal Phase Oil-in-Water Pickering Emulsions Stabilized by Chitin Nanofibrils : 3D Structuring and Solid Foam

Published in:
ACS Applied Materials and Interfaces

DOI:
10.1021/acsami.9b23430

Published: 04/03/2020

Document Version
Publisher's PDF, also known as Version of record

Please cite the original version:
Zhu, Y., Huan, S., Bai, L., Ketola, A., Shi, X., Zhang, X., Ketoja, J. A., & Rojas, O. J. (2020). High Internal Phase Oil-in-Water Pickering Emulsions Stabilized by Chitin Nanofibrils : 3D Structuring and Solid Foam. *ACS Applied Materials and Interfaces*, *12*(9), 11240-11251. https://doi.org/10.1021/acsami.9b23430

ACS APPLIED MATERIALS & INTERFACES

High Internal Phase Oil-in-Water Pickering Emulsions Stabilized by Chitin Nanofibrils: 3D Structuring and Solid Foam

Ya Zhu,[†] Siqi Huan,[†] Long Bai,* Annika Ketola, Xuetong Shi, Xiao Zhang, Jukka A. Ketoja, and Orlando J. Rojas*

Cite This: *ACS Appl. Mater. Interfaces* 2020, 12, 11240−11251

Read Online

ACCESS | Metrics & More | Article Recommendations | Supporting Information

ABSTRACT: Chitin nanofibrils (NCh, ∼10 nm lateral size) were produced under conditions that were less severe compared to those for other biomass-derived nanomaterials and used to formulate high internal phase Pickering emulsions (HIPPEs). Pre-emulsification followed by continuous oil feeding facilitated a "scaffold" with high elasticity, which arrested droplet mobility and coarsening, achieving edible oil-in-water emulsions with internal phase volume fraction as high as 88%. The high stabilization ability of rodlike NCh originated from the restricted coarsening, droplet breakage and coalescence upon emulsion formation. This was the result of (a) irreversible adsorption at the interface (wettability measurements by the captive bubble method) and (b) structuring in highly interconnected fibrillar networks in the continuous phase (rheology, cryo-SEM, and fluorescent microscopies). Because the surface energy of NCh can be tailored by pH (protonation of surface amino groups), emulsion formation was found to be pH-dependent. Emulsions produced at pH from 3 to 5 were most stable (at least for 3 weeks). Although at a higher pH NCh was dispersible and the three-phase contact angle indicated better interfacial wettability to the oil phase, the lower interdroplet repulsion caused coarsening at high oil loading. We further show the existence of a trade-off between NCh axial aspect and minimum NCh concentration to stabilize 88% oil-in-water HIPPEs: only 0.038 wt % (based on emulsion mass) NCh of high axial aspect was required compared to 0.064 wt % for the shorter one. The as-produced HIPPEs were easily textured by taking advantage of their elastic behavior and resilience to compositional changes. Hence, chitin-based HIPPEs were demonstrated as emulgel inks suitable for 3D printing (millimeter definition) via direct ink writing, e.g., for edible functional foods and ultralight solid foams displaying highly interconnected pores and for potential cell culturing applications.

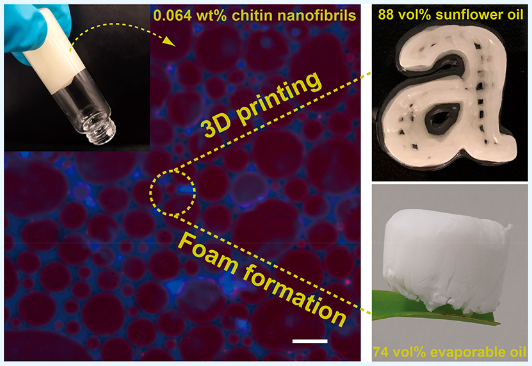

KEYWORDS: *chitin nanofibrils, high internal phase emulsion, Pickering emulsions, porous materials, material molding, direct ink writing*

■ INTRODUCTION

High internal phase emulsions (HIPEs) generally refer to those containing a volume fraction of the dispersed phase $\varphi > 74\%$.[1] They display a large surface area per volume of the continuous phase,[2] which affects uniquely their flow behavior.[3] Hence, HIPEs have become a suitable choice in food products,[4] tissue engineering,[5] multiphase soft materials,[6] and porous material template.[7] Emulsions are kinetically stabilized by surfactants,[8] which are used in high loadings in the case of HIPEs.[9] This is problematic given the possible impacts to the environment,[10] which limits their applications. However, emulsions can be also stabilized with colloidal particles,[11,12] via Pickering stabilization, which is effective in preventing droplet coalescence because of the strong interfacial mechanical barrier generated by the particles.[13] Compared with those stabilized by surfactants, Pickering emulsions offer superior stability at relative low addition of the particles.[14] This is due to the irreversible adsorption of the latter at oil/water interfaces. Therefore, such high internal phase Pickering emulsions (HIPPEs) are preferred over those stabilized by amphiphile molecules,[15] for instance, in the formulation of cost-effective and environmentally friendly systems displaying superior storage stability.[16] Moreover, HIPPEs can be readily used to generate porous materials,[2,17,18] wherein the particles form a template or scaffold.[19]

Biobased particles and colloids have been used to stabilize HIPPEs;[20−23] however, most often, they require surface modification,[24−26] limiting them as alternatives to other colloidal systems.[27] Moreover, there are reasons to raise concerns in the application of HIPPEs in pharmaceutical and food products, which demand particles suitable for clean-labeling, nontoxicity, biocompatibility, and biodegradability.[28] A number of suitable systems has been used to achieve such a goal, including globular proteins,[29−32] zein-based particles,[33]

Received: December 27, 2019
Accepted: February 10, 2020
Published: February 10, 2020

https://dx.doi.org/10.1021/acsami.9b23430
ACS Appl. Mater. Interfaces 2020, 12, 11240−11251

and starch particles.[34] Accessibility, cost-efficiency, and abundance are main factors in any effort to use natural nanoparticles as replacement of synthetic counterparts.[35] Considering this scenario, biomass-derived nanoparticles are ideal candidates for green HIPPEs. For example, HIPPEs with 80% of the internal phase have been stabilized by octenyl succinic anhydride-modified cellulose nanocrystals (OSA-CNCs).[36] However, despite the fact that CNCs are renewable, their grafting with food-grade OSA was required to achieve hydrophobicity. CNCs coated with cationic bovine serum albumin have also been reported in HIPPEs with 80% of the internal phase,[37] which limited the system to being pH-specific, restricting the use. So far, unmodified CNC for HIPPE has been reported by Capron at al., who achieved the stabilization of a nonedible oil.[38] In such a system, salt was added to promote CNC adsorption on the surface of the oil droplets. Therefore, a demand exists for HIPPEs incorporating all clean-label components at minimal loading, including the stabilizer and the oil. In this respect, chitin, an insoluble polymer of N-acetylglucosamine and one of the most abundant resources in nature, stands out for being food-grade, biodegradable, biocompatible, and nontoxic. Although chitin can be resourced from insects and fungi, it is most often extracted from seafood residuals.[39] Chitin nanocrystals (ChNC) obtained by hydrochloric acid hydrolysis have been considered as a Pickering stabilizer for hexadecane-in-water HIPPEs.[40] However, such efforts were limited by the selection of a nonedible oil and the need for salt addition; thus, the possibility remains open to adapt other types of chitin-derived nanomaterials for the purpose of HIPPEs. Only a few reports exist in relation to related efforts.[41−43]

There are many reasons for considering chitin in emulsion stabilization. Individual nanofibril-like chitin is originally assembled as bundles via strong hydrogen bonding, and can be readily isolated by a two-step protocol that involves partial deacetylation and mechanical nanofibrillation,[44] resulting in positively charged chitin nanofibrils (NCh). The disintegration of chitin in acidic condition facilitates the deconstruction by electrostatic repulsion due to the protonation of cationic amine groups, naturally present in deacetylated chitin.[45] Moreover, the residual hydrophobic N-acetyl groups are randomly distributed on NCh, as a result of the deacetylation, which is not site-specific (nonselective),[41] resulting in an increased wettability of NCh at the interface and thus favoring Pickering stabilization.[42] Our recent study discussed NCh at low loading level (0.5 wt % in aqueous phase) as an efficient stabilizer of Pickering emulsions with 50% sunflower oil, yielding long-term stability.[41]

Overall, progress in the area of HIPPEs hinges on the anticipation of the adoption of fully green components, e.g., minimally modified chitin nanofibrils and food-grade oils, which are generally more difficult to be stabilized in emulsions, given their high viscosity and relatively high interfacial tension with water. Herein, we report a two-step approach to produce HIPPEs stabilized solely by naturally derived chitin nanofibrils. The oil phase consisted of an edible oil (sunflower oil), which was used as the internal phase at a volume fraction as high as 88%. Remarkably, the loading of NCh was as low as 0.064 wt % in the system (based on the total mass of the emulsion). The stabilization mechanism is hypothesized by a dual function of NCh in the HIPPEs: adsorption at the oil/water interface in close-packed layers on the droplets, and excess NCh structuring a network in the continuous phase. The prepared HIPPEs are introduced for their versatility in molding and in sustaining compositional changes of the internal phase. From the HIPPEs, we synthesize 3D edible structures using predesigned molds or via 3D printing (direct ink writing, DIW). By changing the internal phase to a volatile mineral oil, we synthesize lightweight NCh-based porous materials. Overall, we offer an alternative for the formulation of HIPPEs that can be considered as core components in green systems. The long-term goal is to use HIPPEs to engineer functional materials.

EXPERIMENTAL SECTION

Materials. α-Chitin was obtained from fresh crabs (*Callinectes sapidus*), which were acquired in the local market (Helsinki harbor, Finland). A purification procedure followed our previous work.[46] The purified, flakelike chitin was stored at 4 °C for further use. NaOH, HCl, 100% acetic acid, Nile red, Calcofluor white stain, and cyclohexane were purchased from Sigma-Aldrich (Helsinki, Finland). Sunflower oil was purchased from a local supermarket. All the chemicals were used as received. Milli-Q water was obtained with a Millipore Synergy UV unit (18.2 MΩ cm) and used throughout the experiments.

Chitin Nanofibril Preparation. Chitin nanofibrils (NCh) was prepared following earlier protocols.[45] Briefly, purified chitin was directly subjected to deacetylation with 33 wt % NaOH solution at 90 °C for 3.5 h. The liquid-to-solid ratio was 25 mL/g. This deacetylation step yielded partially deacetylated chitin (DE-chitin) with a degree of deacetylation of ca. 27%.[41] Afterward, DE-chitin was washed with distilled water to reach neutral pH and further dried at room temperature. Before mechanical nanofibrillation, DE-chitin was redispersed in Milli-Q water at a concentration of 0.2 wt %, following by pH adjustment (3.0) with acetic acid under vigorous stirring. The obtained coarse chitin suspension was homogenized into fine fibrils using a high-speed digital homogenizer (T-25 Ultra-Turrax, IKA, Germany). Ultrasonication was further applied to the fine suspension using a titanium tip sonicator (Sonifier 450, Branson Ultrasonics Co., Danbury, CT, U.S.A.) for 40 min at a power level set at 50% strength with alternating on−off cycles (5−2 s, respectively).

Chitin Nanofibril Characterization. *Microstructure.* The morphology of NCh was observed by transmission electron microscopy (TEM, JEM-2800, JEOL, Japan). A drop of diluted NCh suspension (0.005%) was deposited on electron microscope grid coated with carbon-reinforced formavar film, and negatively stained by uranyl acetate solution before drying at room temperature. Observation was conducted at an acceleration voltage of 120 kV.

ζ-Potential. The electrostatic charge of NCh in aqueous suspensions at given pH (3 to 6) and 25 °C was measured using a Zetasizer Nano (Malvern Instruments Ltd., UK). The pH was adjusted by using 1 M NaOH and 1 M HCl. Prior to measurements, the samples were diluted with buffer solutions (same pH as the samples) to avoid multiple scattering effects.

Interfacial Wettability. Three-phase contact angel (CA) was measured to characterize the wettability of NCh at the oil/water interface. The CA of a captive sunflower oil droplet (5 μL) immersed in water (Milli-Q water) underneath a thin NCh film was determined by using an optical tensiometer (Attension Theta, Biolin Scientific, Finland) with the captive bubble method.[47] Briefly, NCh suspensions at different pH values (3 to 6) were spin-coated onto freshly cleaned mica prior to measurement. Before testing, the obtained film was equilibrated in water for 10 min before releasing the oil droplet. Once the droplet reached the surface of the film, the shape of the droplet was recorded for 2 min with a digital camera. The CA is reported as the angle between solid film and water (surrounding the droplet), indicating the water wetting ability. All measurements were performed under 50% humidity at room temperature.

HIPPE Preparation. A two-step approach including Pickering pre-emulsification followed by continuous oil feeding was applied to prepare the oil-in-water HIPPEs. Briefly, the first step involved the

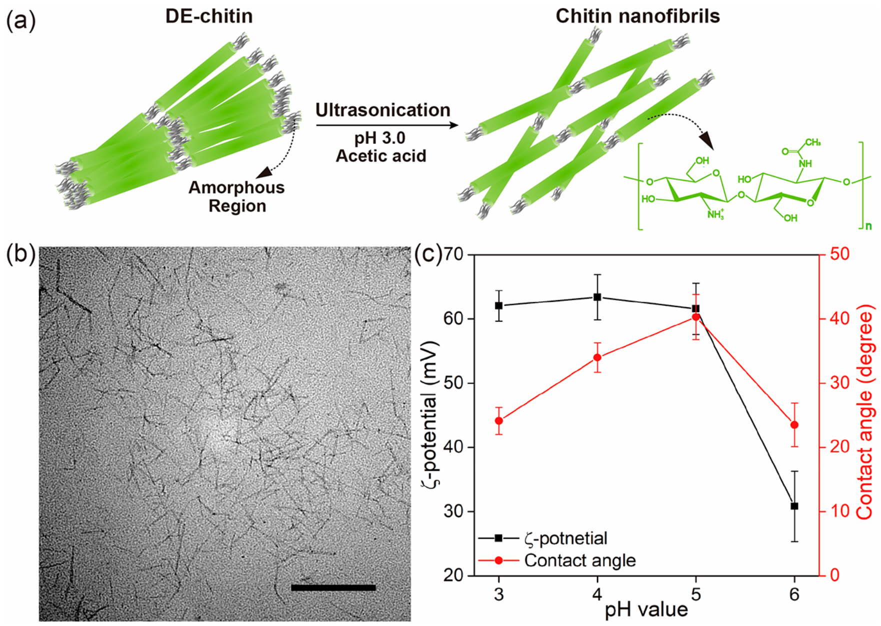

Figure 1. (a) Schematic illustration (not to scale) of the production of chitin nanofibrils (NCh): untreated, never-dried chitin, that is, the deacetylated chitin in the absence of any mechanical treatment, is produced in the form of small flakes. The NaOH-induced deacetylation leads to structures comprising noncharged microfibrils, which are tightly bundled, particularly after removing extra water. Such material is insoluble and nondispersible in water. However, the deacetylated chitin can be resuspended into water at pH 3 (with acetic acid), wherein surface amines are fully protonated by the development of positively charges. Under proper mechanical treatment, the bundled chitin structures are effectively disintegrated into chitin nanofibrils, as shown. (b) TEM image of NCh initially suspended in water (pH 3). The scale is 500 nm. (c) ζ-potential (black square) and three-phase contact angle (red circle) of NCh at pH values from 3 to 6 (Note: at high pH conditions, the possible effects of association or aggregation of NCh should be considered in the measurements and for the intended uses). All measurements were performed at room temperature.

preparation of emulsions with 66% of the oil phase. For this, 7.5 mL of NCh aqueous suspension (0.5 wt %) and 15 mL of sunflower oil were mixed at 22 000 rpm for 1 min using a high-speed digital homogenizer (T-25 Ultra-Turrax, IKA, Germany). Afterward, aliquots of 2 mL of sunflower oil were continuously added while blending at 11 000 rpm until the desired internal phase fraction was achieved. The final concentration of NCh according to the total weight mass was 0.064 wt %. Images of HIPPEs were acquired after storing the samples for 24 h. Long-term stability was monitored and photographed after storage for 14 days. All HIPPEs were kept at room temperature.

To visualize simultaneously NCh and sunflower oil, we stained sunflower oil with Nile red before HIPPE preparation. Nile red solution (1 mg/mL in ethanol) was thoroughly mixed with sunflower oil at a ratio of 1/25 overnight. A similar preparation procedure was used to produce stained HIPPEs. The stained samples were stored at 4 °C before characterization.

HIPPE Characterization. *Droplet Sizing.* To measure the droplet size, we observed HIPPEs at different oil concentrations using optical microscopy (Leica DM 750, Leica, Germany) with a 10× objective lens. A drop of HIPPE was dripped onto a microscope slide and covered with a glass coverslip (Assistent, Sondheim, Germany). The droplet size was determined from optical microscopic images (at different magnifications) via ImageJ software (imagej.nih.gov) by counting at least 200 droplets.[48]

Rheology. The viscosity of HIPPEs was measured using a rheometer (MCR 302, Anton Paar, Germany) equipped with a parallel plate (PP25) and a gap fixed at 0.5 mm. All HIPPEs were presheared at a shear rate of 10 s^{-1}. The shear viscosity was monitored at varying shear rates (0.01 to 100 s^{-1}). For dynamic viscoelastic measurements, the linear viscoelastic range was determined with a strain sweep (0.01 to 100%) at a fixed frequency of 10 rad/s. After this, a dynamic frequency sweep (0.1 and 100 rad s^{-1}) was conducted on the rheometer using the parallel plate geometry (PP25) with a gap fixed at 0.5 mm and by applying a constant strain of 1.0%, which was within the nearly linear region. The dynamic spectra were obtained by recording the storage (G') and loss (G'') moduli as a function of frequency. To determine the yield stress of HIPPE at 88% oil fraction, we carried out oscillatory measurements at a constant frequency of 1 Hz and increasing stress from 1×10^{-2} to 10^2 Pa. All measurements were performed at 25 °C.

Observation of HIPPE Droplets. The HIPPE droplets were examined using confocal laser scanning microscopy (CLSM) with a 40× objective lens (Leica DMRXE, Leica, Germany). The oil droplets were gently collected from the top layer of the HIPPEs by using a pipet since no creaming, sedimentation or oiling-off occurred in none of the samples. One hundred microliters of the oil droplets were stained with 10 μL of Nile red solution prior to observation. After homogeneously mixing with a pipet and equilibrating for 10 min at room temperature, 6 μL of dyed samples were placed on a microscope slide and covered with a glass coverslip without squeezing the assembly. The coverslip was quickly fixed by nail polish to avoid evaporation. The excitation and emission spectrum for Nile red are 488 and 539 nm, respectively.

Multichannel fluorescent microscopy (Zeiss Axio Observer optical microscope, Zeiss, Germany) was used to simultaneously visualize NCh and sunflower oil in HIPPEs. A 63× oil immersion objective was used for all sample imaging. Sunflower oil was stained with Nile red prior to HIPPE preparation and NCh was stained by Calcofluor white for observation. All the sample preparation procedure was similar as that used for CLSM. The excitation and emission spectra for Calcofluor white stain are 365 and 435 nm, respectively. Merged fluorescent images were processed by ImageJ.

To assess the structure and morphology of oil droplets in situ, we conducted cryogenic microscope observation with a scanning electron microscope (S4800 FESEM, Hitachi, Japan) using liquid nitrogen to freeze the sample in the preparation and for cryo-transfer. Briefly, a drop of HIPPE was placed in a specimen holder and immediately immersed in liquid nitrogen. Afterward, the sample was transferred to the preparation unit of the cryo-SEM wherein the temperature was −160 °C and the pressure was 1×10^{-6} mbar. After fracturing the sample with a blade, a layer of Au was sputter-coated onto the sample. The sample was inserted into the observation chamber equipped with

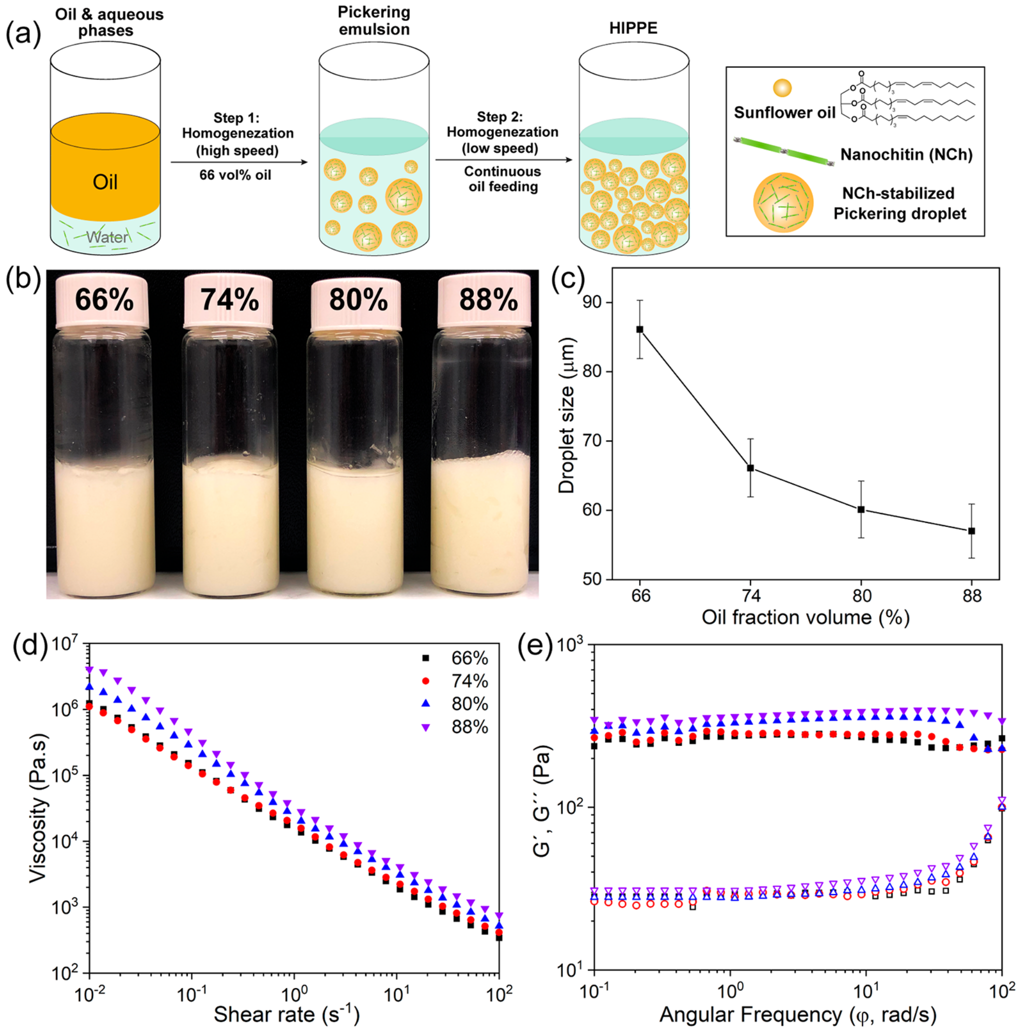

Figure 2. (a) Schematic illustration (not to scale) of the two-step fabrication of high internal phase Pickering emulsion (HIPPE) using NCh suspension and sunflower oil. (b) Visual appearance and (c) droplet size of HIPPEs with sunflower oil volume fraction of 66 to 88%. The pH of the NCh aqueous suspension is 3. The oil fraction volume in (b) is indicated on top of each sample. (d) Shear thinning and (e) moduli of HIPPEs at different oil volume fractions. The storage (G') and loss (G'') moduli are indicated with filled and open symbols, respectively.

a SEM cold stage module held at −140 °C throughout the measurement.

Application of HIPPEs. *Generation of Predesigned Shapes.* The moldability of the HIPPEs (0.064 wt % NCh at 88% sunflower oil) was demonstrated by fabricating a three-dimensional object using direct cutting of the freshly prepared HIPPEs. The HIPPE was also used as a printable ink for DIW-based 3D printing (BIO X, CELLINK, Sweden) with a pneumatic printing head. The device utilized 3 mL pneumatic syringe provided by CELLINK and sterile blunt needles (plastic, Drifton, Denmark). The nozzle size of the needle was 0.51 mm for all samples. Given designs were printed on a plastic Petri dish using rectilinear infill patterns and 10−25% infill density. Based on an initial optimization, the moving speed of the printhead was 8 mm s^{-1}, the extrusion speed was 0.012 mm s^{-1}, and the extrusion pressure was controlled in the range of 20−40 kPa. Photographs of different shapes were taken at least 1 h after generation.

Porous Materials. To prepare all-NCh solid foams using HIPPE as a template, we replaced the sunflower oil by cyclohexane. The procedure for preparation of cyclohexane-in-water HIPPE was the same as that used for sunflower oil. The concentration of NCh in the continuous phase was 0.5 wt %. The final cyclohexane loading in this study was over 74%. Afterward, freshly prepared HIPPE sample was freeze-dried at least 2 days to obtain a porous material. The morphology and structure of the porous material was observed by SEM (Zeiss Sigma VP, German) operated under vacuum and at an accelerating voltage of 2 kV. The samples were coated with a thin layer of platinum (3 nm) using a high-vacuum sputter coater (Leica EM ACE600) before imaging.

■ RESULTS AND DISCUSSION

Chitin Nanofibril Properties. Chitin nanofibrils (NCh) were prepared by mechanical disintegration from deacetylated chitin (DE-chitin) under acidic condition, as shown schematically in Figure 1a. The nanofibrillation process simultaneously exposed amine groups of deacetylated chitin, resulting in positively charged NCh. Because deacetylation of N-acetyl groups is nonspecific, a random distribution of amino groups in NCh was expected. TEM micrograph of NCh initially dispersed in aqueous media indicated well-dispersed fibril-like particles, with no signs of aggregation (Figure 1b). The NCh lateral size was close to that of individual chitin nanofibrils (∼10 nm).[49] This is attributed to the electrostatic repulsion originated from the highly charged surface of NCh (Figure 1c), as well as the strong mechanical deconstruction during nanofibrillation. The aspect ratio (length/width, L/w) of NCh was calculated to be ∼16, which is similar to the value reported earlier.[41] It should be noted that drying effects during

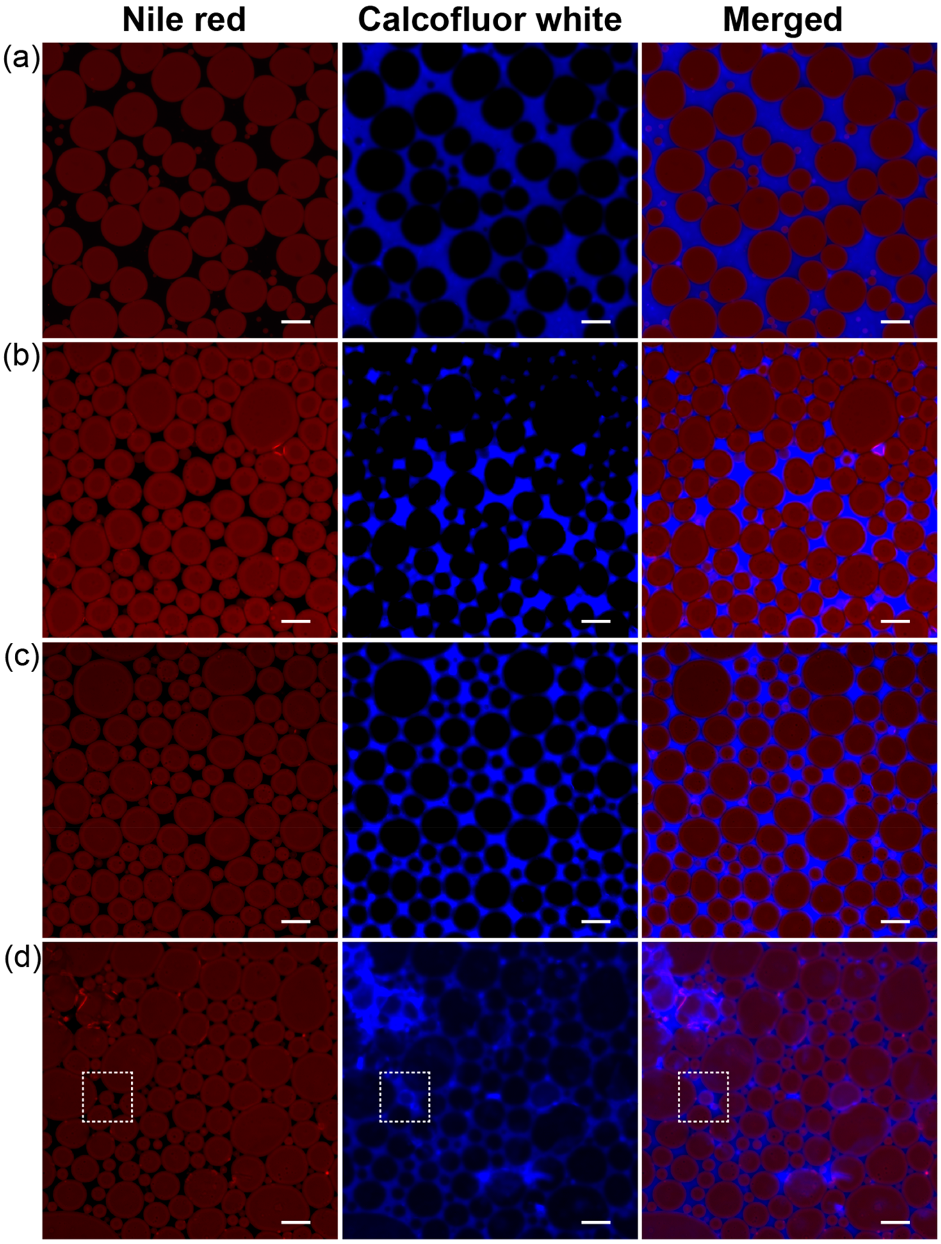

Figure 3. Fluorescent micrographs (multichannel fluorescent microscopy) of HIPPEs stabilized with NCh (pH 3) at oil volume fractions of (a) 66, (b) 74, (c) 80, and (d) 88%. The concentration of NCh in continuous phase is 0.5 wt %. The left, middle, and right rows correspond to the stained oil phase, dyed NCh, and merged images, respectively. The dashed boxes in d indicate the contour of oil droplets. The scale bar is 100 μm. All samples were stored at room temperature for 24 h prior to observation.

TEM imaging to assess the NCh morphology may obscure or cause associated artifacts. Any interpretation should keep this in mind. NCh was easily produced under conditions that are less severe compared to those that apply to typical biomass-derived nanoparticles, such as nanocelluloses.

Because the protonation of amine groups is pH-dependent, the properties of NCh can be tuned by pH shifts of the aqueous medium. As shown in Figure 1c, the ζ-potential of NCh in the interval of pH between 3 and 5 was fairly constant, approximately +60 mV, but it sharply became less negative, less than +30 mV, at pH above 6, which can be attributed to the deprotonation of surface amino groups. Translucent, homogeneous, and less-surface-active NCh suspensions were observed at pH ≤5 (Figure S1); however, a nonhomogeneous suspension with a large number of trapped bubbles was observed at pH 6, which was caused by aggregated NCh in the medium.

The interfacial wettability of NCh, affecting Pickering emulsion stabilization, was investigated via three-phase contact angle (CA) (Figure 1c). The aqueous phase contacted the NCh film first before a captive oil drop was released underneath the film surface (Figure S2). The CAs measured between NCh film and water increased from 24° to 40° by increasing the pH from 3 to 5, that is, the originally hydrophilic NCh surfaces become hydrophobic as the pH increased. This is ascribed to the more limited protonation of surface amino groups of NCh at higher pH (Figure 1c). Interestingly, the CA decreased to 23° at pH 6, which is likely a result of partial aggregation of NCh in the suspension and the high viscosity, both of which limited the homogeneity of spin-coated film.

The results indicate that the hydrophobicity of NCh can be tailored by changing the pH of the aqueous phase, which should be less than 6 to stabilize NCh-based HIPPEs. Overall, fine chitin nanofibrils bearing tunable surface properties were reproducibly obtained by mechanical disintegration, making them a promising alternative to biomass-derived systems for the formulation of green HIPPEs.

NCh-Stabilized HIPPEs. *Formation of HIPPE.* The two-step preparation protocol to produce NCh-stabilized HIPPEs is shown in Figure 2a. This method allows control on the properties of Pickering pre-emulsions, which is a key factor to tune the performance of the final HIPPEs. The HIPPEs stabilized by NCh at different oil fractions (pH 3) were homogeneous and free of oiling-off (Figure 2b), even at 88%, implying that the two-step approach is efficient in producing fine NCh-stabilized HIPPEs. Moreover, the NCh concentration used in the continuous phase was 0.5 wt % (0.064 wt % based on total mass, for 88% oil fraction), which is considerably lower than in an earlier effort with edible oil stabilized with protein microgels.[50] Other protein-based HIPPEs have been achieved at lower loading with protein particles.[32] The results overall indicate the excellent ability of NCh in stabilizing HIPPEs, especially if one considers the sources, cost, and flexibility in tailoring the size and charge characteristics of the material. This applies to edible oils that are typically more challenging, given the high viscosity and the interfacial tension with water, which is usually lower than that of nonedible oils. The effect of NCh as HIPPE stabilizer may result from a combination of different features: (a) preference of NCh for less polar oils, determined by the inherent hydrophilicity of NCh;[51] (b) improved interfacial wettability; and (c) the compliance of NCh at the interface.[41] The droplet size was determined by counting droplets from optical micrographs at different magnifications (see histograms in Figure S3), and presented a decreasing trend with the oil volume fraction (Figure 2c). The average droplet size of emulsions prepared with 74, 80, and 88 vol % oil was similar, ∼60 μm. This is likely due to the extended time of agitation used in HIPPE preparation. Initially, the Pickering pre-emulsion at 66% oil volume fraction showed large droplets, which were caused by the insufficient breaking power of the homogenizer to reduce the bulk oil phase into small droplets. Afterward, the breakdown of the oil phase was increased by the stepwise addition of the oil to the pre-emulsion, which involved extended agitation time upon oil loading and resulted in a reduction in drop size. On the other hand, the newly formed droplets in the second emulsification step, following continuous oil loading, may also contribute to the smaller population of oil droplets observed because of the small volume of oil phase that is added in each interval.

Oil droplets produced from NCh suspension at pH 3 at different oil fractions were well dispersed in the aqueous phase after 24 h storage, and showed similar droplet size as measured by optical micrographs (Figure S4). Figure S4 also clearly shows crowding of oil droplets after exceeding a high-internal-phase limit. In comparison with common HIPEs that display deformation of the dispersed droplets into polyhedrical structures,[52] no significant changes in droplet shape were observed for NCh-stabilized HIPPEs. The high packing level is attributed to the polydispersity of droplet size in HIPPEs. Indeed, the maximum volume packing for spheres of the same size is 74%; deformation of oil droplets is a means to stabilize emulsions with higher oil volume fractions. In our HIPPEs, the droplets showed a wide size range after reaching the threshold (Figures S3 and S4), so that smaller oil droplets fit between larger ones, facilitating effective droplet packing. It should be noted that slight deformation of oil droplets was observed in the emulsions with more than 80 vol % oil (Figure S4).

The microstructure of droplets and their location in the continuous phase as well as that of NCh were followed by multichannel fluorescent microscopy. In the merged images, the continuous phase is shown in blue for the HIPPEs at all oil volume fractions tested (Figure 3). There is a clear indication that NCh is distributed in the continuous, aqueous phase (Figure 3a). Furthermore, entangled, randomly distributed, and self-connected NCh is clearly observed, which indicates that the stabilization of HIPPEs might partially originate from NCh structuring in the aqueous phase (Figure S5). Despite the contribution to dye reflection from the aqueous phase, blue contours around the oil droplets were clearly identified, ascribed to adsorbed NCh (Figure 3d and Figure S5). This is a direct evidence that NCh adsorbs at the oil/water interface, a topic that will be discussed in the next section.

We further investigate the influence of the pH of the NCh suspension on the formation of HIPPEs (Figure S6). HIPPEs stabilized by NCh at a pH in the range between 3 and 5 showed similar visual appearance at 88% oil volume fraction. At pH 6, the emulsion broke soon after preparation (Figure S6a), which is explained by the aggregation of NCh nanoparticles given the weak electrostatic repulsion (less protonation) (Figure 1c). Observing the structure of the samples (Figure S6b), the stability decreased when changing the pH from 3 to 5. Although NCh was stable against aggregation and three-phase contact angles proved a better interfacial wettability of NCh to the oil phase at higher pH (Figure 1c), the lower interdroplet repulsion facilitated coarsening at high oil loading (see sample at pH 5 in Figure S6b). On the other hand, the change in surface properties may also impair network formation in the aqueous phase, which is key to achieving fine HIPPE droplets. As a conclusion, the preparation of HIPPEs with NCh should consider the effect of the pH of the suspension.

The rheology of NCh-stabilized HIPPEs is shown in Figure 2d, e. From Figure 2d, all emulsions showed a typical shear-thinning behavior. The apparent viscosity increased with the oil volume fraction, as expected from the shorter interparticle distance and interdroplet friction (Figure 3 and Figure S4), which restricted droplet flow. Figure 2e shows the viscoelasticity of HIPPEs at different oil volume fractions, and all emulsions displayed an elastic behavior, that is, a higher storage modulus (G'). Furthermore, we observed that the formed HIPPEs were not readily dispersed in water, which can be attributed to the relatively low NCh loading and the bridging in oil droplets, forming an interconnected network that resist their dispersion. These effects are expected in the formation of emulsion gels, rather than normal concentrated emulsions. Similar to the viscosity, the increased oil fractions slightly increased the G' of HIPPEs, owing to a denser packing of oil droplets within the internal phase.[53,54] On the other hand, the presence of free NCh in the continuous, aqueous phase may promote the formation of physical networks (Figure 3 and Figure S5), contributing to the elastic behavior of HIPPEs.[41] As indicated above, such HIPPEs show a great potential in foodstuff, particularly in oil-rich compositions. On the basis of the rheological tests, the prepared NCh-stabilized HIPPEs present similar properties (appearance and texture) as

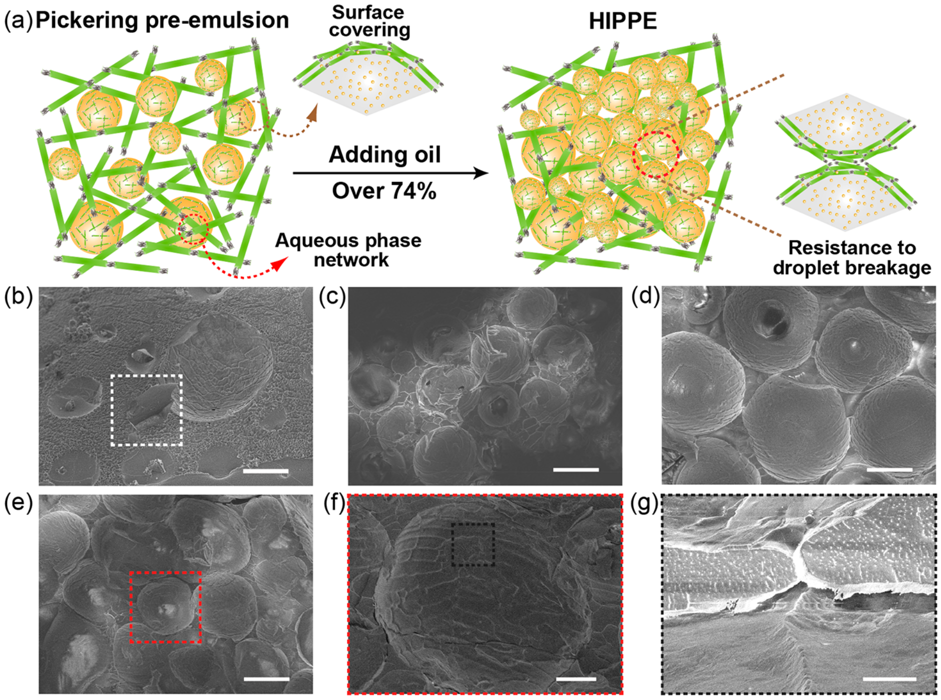

Figure 4. (a) Schematic illustration (not to scale) showing the stabilization mechanism of HIPPEs stabilized by NCh. Cryogenic scanning electron microscope images of HIPPE droplets stabilized by NCh (pH 3) at oil volume fraction of (b) 66, (c) 74, (d) 80, and (e) 88%. The concentration of NCh in continuous phase is 0.5 wt %. (f, g) Enlarged microscopic images of HIPPE droplet at 88% oil volume fraction in e. The white dashed box in a is used to highlight a flakelike NCh sheet. The red and black dashed boxes indicate selected locations for magnification. The scale bar is (b−e) 50, (f) 25, and (g) 2 μm.

margarine[55,56] and mayonnaise,[57] thereby indicating the possibility for HIPPEs as a substitute for related formulations.

Stabilization Mechanism. For most of emulsions, the gel-like behavior is expected to improve the stability.[35] However, as discussed above, all HIPPEs prepared from NCh suspensions at different pH showed similar gel-like properties (Figure S6) but displayed a significantly different droplet structures. This indicates that other factors also play a role in the stability and microstructure of NCh-stabilized HIPPEs. According to the results, a stabilization mechanism for HIPPEs that is originated from dual functions of NCh is proposed, as shown in Figure 4a: (1) NCh structuring in the aqueous phase to form deformable, strong networks surrounding the oil droplets throughout HIPPE formation, preventing oil droplets approaching and coarsening, and (2) stabilizing the oil droplets by forming an adsorbed layer that inhibits the breakage and coalescence of oil droplets. It should be also noted that the Pickering pre-emulsion droplets formed in the first step may also act as a secondary stabilizer of the subsequently added oil phase, a common feature in two-step emulsification systems.

Cryo-SEM was used to directly visualize the morphology of the oil droplets in the HIPPEs (Figure 4). As shown in Figure 4b−e, the shape and distribution of oil droplets at different oil volume fractions show similar trends as those concluded from Figure 3 and Figure S5. As shown in Figure 4b, flakelike NCh sheets were identified from the micrograph (see the white dash-line box), indicating that upon generating the Pickering pre-emulsions, fibril-like NCh structured as a network in the aqueous phase. Ice crystals were observed, given that no sublimation occurred during sample preparation (Figure 4b). Increasing oil loading over 74%, sheet- or fiberlike structures involving NCh could still be observed in the images (Figure 4c−e), particularly from Figure 4f.

In separate experiments, we used cyclohexane to facilitate freeze-drying of the respective HIPPEs. Thus, after removing the oil and water phases, a porous solid formed, displaying fibrous webs of NCh (Figure 7d). It is reasonable to assume that such a network initially surrounds the oil droplets in the aqueous phase and facilitates the stabilization upon oil loading in the Pickering pre-emulsion. For HIPPE preparation, the oil phase was added continuously into the pre-emulsion, keeping the same volume of water. Thus, the concentration of NCh in the aqueous phase is the same for both emulsions with oil vol % of 66 or 88%. This raises the question whether the initial network structure in the aqueous phase determines the formation and stability of HIPPEs. To test this hypothesis, we used a lower NCh concentration (0.3 wt %) to produce the HIPPEs using the two-step process. The pre-emulsion containing 66% oil was obtained successfully. However, the emulsions with >74% oil fraction were not stable, suggesting that relatively low NCh loading is insufficient to generate Pickering pre-emulsion droplets, for example, by interfacial adsorption, and to enable sufficient structuring during pre-emulsification. This result highlights that the initial network structure plays a key role in stabilizing HIPPEs. As an extension of previous discussion, NCh of longer axial aspect (produced via microfluidization[46]) was applied at 0.3 wt % in the aqueous phase (Figure S7). Pickering pre-emulsions and HIPPE at 88% oil fraction were successfully obtained, with a similar droplet structure as that observed for HIPPEs at 0.5 wt % aqueous phase concentration of the shorter NCh, Figure S7a, b. The results clearly indicate a better structuring of long NCh, even at relatively lower concentrations.[41] In sum, NCh is structured in the aqueous phase of the HIPPEs, generating a “scaffold” during pre-emulsification and increasing the elasticity, which arrest droplet mobility and coarsening. A

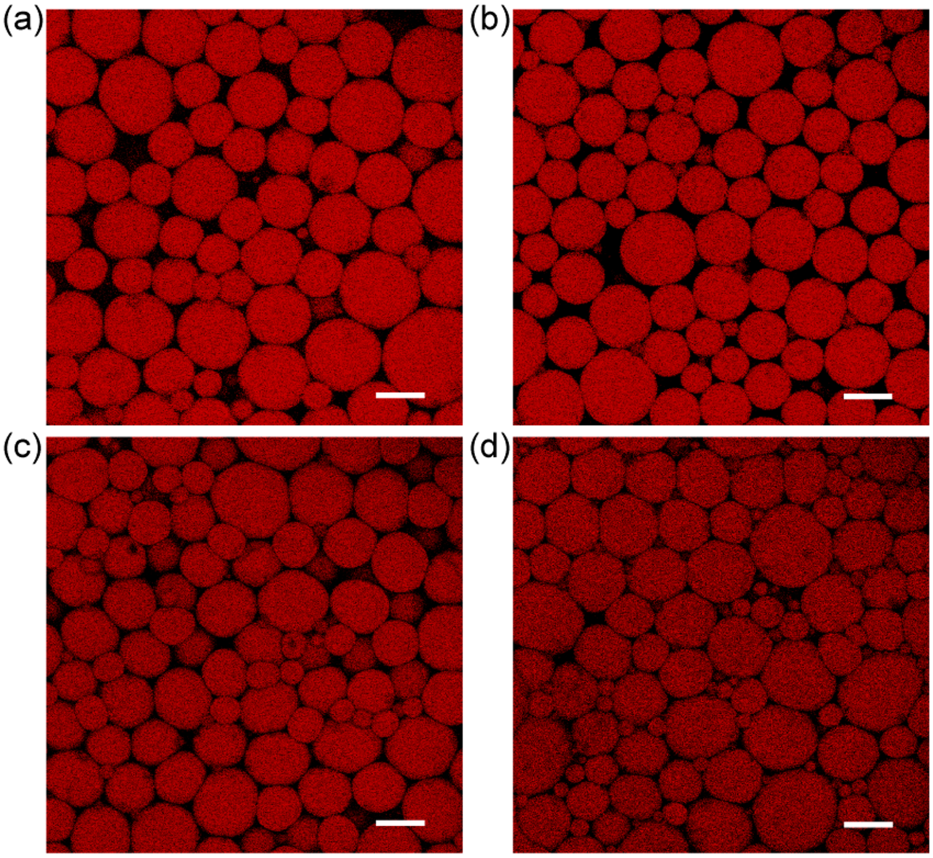

Figure 5. Confocal images of HIPPEs stabilized by NCh (pH 3) at oil volume fraction of (a) 66, (b) 74, (c) 80, and (d) 88%. The concentration of NCh in continuous phase is 0.5 wt %. All emulsions were stored at room temperature for 14 days. The oil phase was dyed by Nile red during emulsion preparation. The pH of NCh suspension was 3 for all sample preparations. The scale bar is 80 μm.

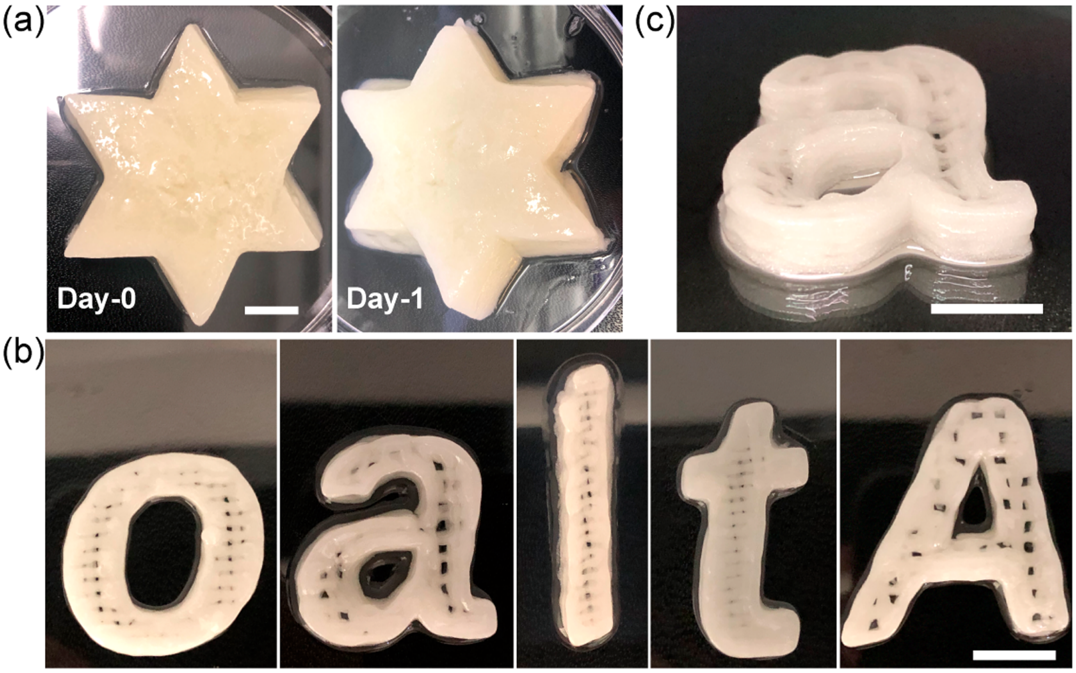

Figure 6. (a) A star object shaped from HIPPE stabilized by 0.064 wt % NCh (pH 3) at 88% oil volume fraction. The HIPPE was freshly prepared before generating the shape. The left photograph was taken 1 h after generation, and right one was taken after storing for 1 day at room temperature. (b) Top view of letters processed using HIPPE at 88% oil volume sample in a. (c) Enlarged side view of letter "a" from b. The images were taken after storing for 1 h at room temperature. The scale bar is 1 cm for a−c.

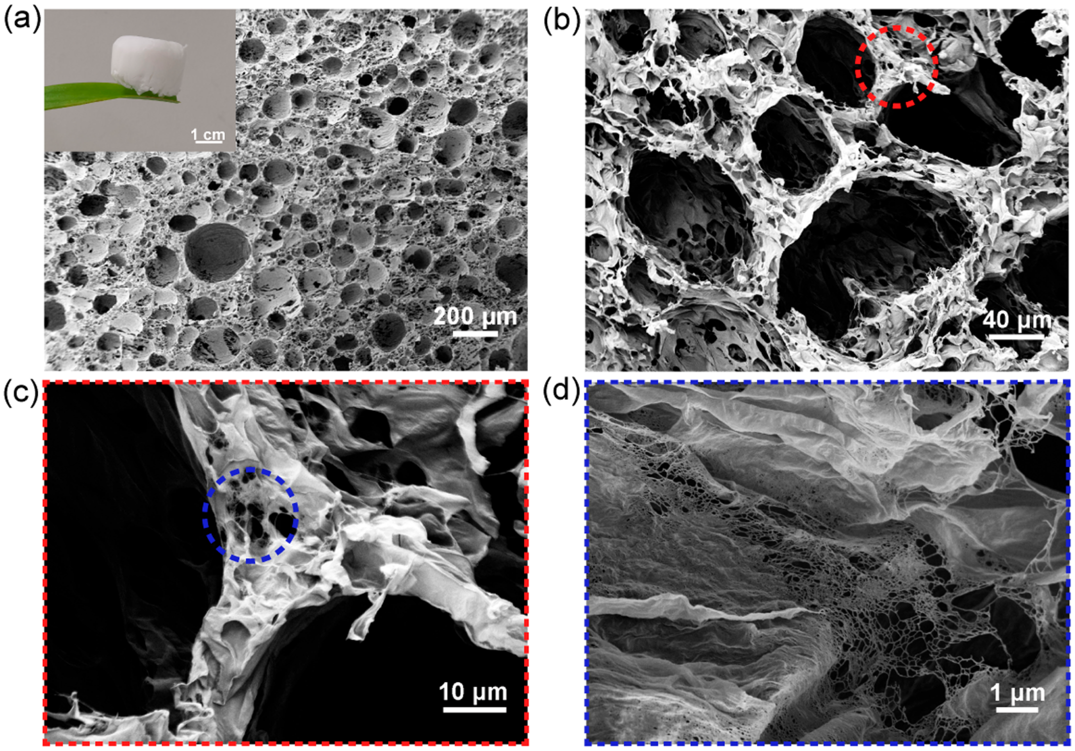

Figure 7. (a−d) SEM images of porous materials produced by freeze-drying HIPPE containing 74% cyclohexane and 0.5 wt % NCh (pH 3) in the continuous phase. The inset in a shows the photograph of the porous material on the leaf of a bracket-plant. (c, d) Enlarged microscopic images of internal porous structure in b. The red and blue dashed circles indicate selected locations for magnification.

trade-off exists between NCh axial aspect and minimum concentrations to stabilize the HIPPEs.

A question that remains is how the high-oil-loaded droplets resist coalescence, even under close packing. As shown in Figure 4g, sheetlike structures indicated that NCh was located on the droplet surface of the HIPPEs, even at low interfacial adsorption (Figure 3d). The adsorbed NCh layer covering the deformed droplets ensures mechanical stability. There is a clear evidence that NCh forms a dense, connected network at the oil/water interface, preventing oil coalescence even at relatively low NCh concentrations or low surface coverage.[41] As a result, the resistance of droplets at 88% oil fraction against coalescence originated from the high efficiency of NCh to form a strong interfacial barrier once NCh adsorbs during emulsification. The synergistic dual function of NCh, namely, structuring in the aqueous phase and formation of an interfacial barrier, determines the stability and structure of HIPPEs.

Storage Stability of HIPPEs. The storage stability is a key factor for practical emulsion applications, particularly for HIPPEs. No significant change (no oiling-off) was observed after keeping the emulsions undisturbed for 2 weeks at room temperature, which indicates that NCh-stabilized HIPPEs are stable against storage even at high oil loadings and low stabilizer addition. As shown in the CLSM images (Figure 5), the oil droplets were distributed homogeneously and kept their shape after 2 weeks, and the droplet size at different oil volume fractions was nearly constant. Moreover, the morphology of the oil droplets and the visual appearance of the HIPPE (88% oil volume) were maintained even after 3-month storage (Figure S8). However, we note that further deformation of the oil droplets at high oil loading was observed upon storage. The high storage stability is caused by (1) irreversibly adsorbed NCh that restricted the coalescence of oil droplets even in close contact, and (2) the elasticity and structure of continuous phase of HIPPEs locked the displacement of oil droplets, preventing creaming, or separation. In conclusion, the high storage stability demonstrates the superior performance of NCh as a naturally derived, unmodified HIPPE stabilizer.

HIPPE Applications. *Moldable Materials.* We first introduce the processability of NCh-stabilized HIPPEs as bulk, moldable material (Figure 6). By using a mold, a star-shaped 3D object was created from the HIPPE with 88% oil fraction, Figure 6a. The structure remained unchanged after 1 day, with little release of oil. This result can be attributed to the high storage modulus of HIPPEs (Figure 2e), as reported for NCh hydrogels.[58] Moreover, the heterogeneous oil droplet size distribution of the HIPPEs may also contribute to an increased strength of the formed gel network. The integrity of oil droplets at high loading is thus confirmed, enabling processability into given shapes.

DIW-based 3D printing was used to generate other complex architectures from the HIPPEs (Figure 6b). The printability of HIPPE with 88% oil was demonstrated by the measured shear thinning (Figure 2d) and yield stress (Figure S9). The HIPPE underwent pronounced shear thinning and the apparent viscosity decreased by several orders of magnitude with the increased shear rate, from 1×10^{-2} to 1×10^{2} s^{-1} (the obtained values fit the demands of typical DIW, e.g., to ensure flow through the deposition nozzle) (Figure 2d). Oscillatory rheological measurement at low strain indicated that the storage modulus (G') of the HIPPE dominated at lower shear stresses, whereas the loss modulus (G'') became more relevant at high shear, after crossing the yield stress point, showing a yield stress of ca. 30 Pa, which is within the range needed for extrusion-based 3D printing (Figure S9).[59] As shown in Figure

6b and Video S1, different letters bearing round structures ("o" and "a"), straight lines ("l" and "t"), and high curvatures ("a", "t", and "A") were printed with high fidelity. In the meantime, different infill densities in the letters were adjusted (see "A" and "t" in Figure 6b), showing the tuneability of HIPPE ink. Furthermore, the layers stacked upon printing are easily discernible when observing, for example, side view of letter "a" (Figure 6c), indicating the ability of HIPPE to create objects with geometrical complexity at the millimeter scale. It should be noted that compared to other hydrogel or emulgel inks, the total solid content in our HIPPE was extremely low,[6,60] indicating the superior printability of HIPPEs. Because NCh-stabilized HIPPE ink included all food-grade components, a strategy for future food manufacturing, 3D printing foods, is advanced in this study.

Porous Materials. The outstanding stability and high processability of HIPPEs allow the fabrication of porous materials that contain bulk macroporous structures. Cyclohexane was used as oil phase to prepare NCh-stabilized HIPPEs, following with freeze-drying to remove water and oil. A large number of pores resulted with the excess NCh forming their walls (Figure 7). The inset in Figure 7a illustrates the lightness of the object, given the extremely low solids content in the precursor HIPPE. Porous materials showing relatively uniform wall thickness and similar pore size as that of the precursor droplets (74% oil phase) were obtained at 0.5 wt % NCh concentration in the continuous phase (Figure 4c). No obvious collapse of the porous structures was observed, implying a high structural integrity (Figure 7b, c), which can be attributed to the interconnectivity of NCh adsorbed during water evaporation,[40,41] and the formation of strong intra- and interhydrogen bonding between NCh.[43] It should be noted that smaller pores were observed (not related with the oil droplets), which resulted from the different evaporation rates for water and cyclohexane during drying. Moreover, the droplet surface that was not fully covered with NCh is a possible source of the smaller open pores formed on NCh walls upon drying. The good mechanical performance of NCh foams relates to that of the native α-chitin nanofibrils.[61] The enlarged view of the structure clearly shows dense, connected fibrous webs surrounding the pores (Figure 7d). Importantly, the use of NCh-stabilized green HIPPE templates addresses the issue raised in relation to biocompatibility and biotoxicity compared to previous studies.[62] Overall, NCh-stabilized HIPPEs are demonstrated as a route to fabricate porous materials with great potential for the construction of supports and scaffolds with possible uses in bioengineering, food and pharma, catalysis, among others.

CONCLUSIONS

Stable oil-in-water, high-internal-phase Pickering emulsions stabilized by chitin nanofibrils were successfully prepared using a simple two-step strategy. The internal phase fraction, comprising an edible sunflower oil, reaches values as high as 88%. Two possible underlying mechanisms for the formation and stabilization of HIPPEs are proposed: (1) structuring continuous phase to form deformable, connected, fibrous network structures upon Pickering pre-emulsification, with oil droplets covered with NCh, which prevents the droplets from approaching each other and arrests coarsening, and (2) irreversible adsorption of NCh at oil/water interfaces, inhibiting coalescence and breakage of oil droplets. Moreover, the formed Pickering pre-emulsion droplets in the first step may also act as a secondary stabilizer for subsequent oil phase emulsification. Substitutes for food products (e.g., margarine) are demonstrated according to the rheological performance. A new manufacturing strategy for edible materials is proposed by combining DIW-based 3D printing and food-grade HIPPEs. Biocompatible, nontoxic porous materials with tunable internal properties were produced by using HIPPE as a template. Our results demonstrate that NCh-stabilized HIPPEs can fulfill the requirement of clean-labels for foodstuff and green materials.

ASSOCIATED CONTENT

Supporting Information

The Supporting Information is available free of charge at https://pubs.acs.org/doi/10.1021/acsami.9b23430.

Visual appearance of chitin nanofibril suspensions at different pH values and corresponding HIPPEs obtained; images from three-phase contact angle measurements; optical images and calculated droplet size; confocal of HIPPEs at different oil fractions; blue channel image of HIPPE at 88% oil fraction; confocal and rheological test of HIPPE using long-fibril NCh; storage stability of HIPPEs after 3 months; and oscillatory rheology of HIPPE at 88% oil fraction (PDF)

Video S1 showing extrusion-based 3D printing (MP4)

AUTHOR INFORMATION

Corresponding Authors

Long Bai − *Bio-Based Colloids and Materials, Department of Bioproducts and Biosystems, Aalto University, Aalto FIN-00076, Espoo, Finland; Departments of Chemical & Biological Engineering, Chemistry, and Wood Science, 2360 East Mall, The University of British Columbia, Vancouver, British Columbia V6T 1Z3, Canada;* orcid.org/0000-0003-3356-9095; Phone: +1-236-869-0416; Email: long.bai@ubc.ca

Orlando J. Rojas − *Bio-Based Colloids and Materials, Department of Bioproducts and Biosystems, Aalto University, Aalto FIN-00076, Espoo, Finland; Departments of Chemical & Biological Engineering, Chemistry, and Wood Science, 2360 East Mall, The University of British Columbia, Vancouver, British Columbia V6T 1Z3, Canada;* orcid.org/0000-0003-4036-4020; Phone: +1-604-822-3457; Email: orlando.rojas@ubc.ca

Authors

Ya Zhu − *Bio-Based Colloids and Materials, Department of Bioproducts and Biosystems, Aalto University, Aalto FIN-00076, Espoo, Finland*

Siqi Huan − *Bio-Based Colloids and Materials, Department of Bioproducts and Biosystems, Aalto University, Aalto FIN-00076, Espoo, Finland; Departments of Chemical & Biological Engineering, Chemistry, and Wood Science, 2360 East Mall, The University of British Columbia, Vancouver, British Columbia V6T 1Z3, Canada*

Annika Ketola − *VTT Technical Research Centre of Finland Ltd, Jyväskylä FI-40101, Finland*

Xuetong Shi − *Bio-Based Colloids and Materials, Department of Bioproducts and Biosystems, Aalto University, Aalto FIN-00076, Espoo, Finland*

Xiao Zhang − *Bio-Based Colloids and Materials, Department of Bioproducts and Biosystems, Aalto University, Aalto FIN-00076, Espoo, Finland*

Jukka A. Ketoja − *VTT Technical Research Centre of Finland Ltd, Jyväskylä FI-40101, Finland;* orcid.org/0000-0002-8260-4267

Complete contact information is available at:
https://pubs.acs.org/10.1021/acsami.9b23430

Author Contributions

[†]Y.Z. and S.H. contributed equally to this work.

Notes

The authors declare no competing financial interest.

ACKNOWLEDGMENTS

The authors acknowledge funding from the European Research Council under the European Union's Horizon 2020 research and innovation program (ERC Advanced Grant Agreement 788489, "BioElCell"). This research was undertaken, in part, thanks to funding from the Canada Research Chairs program and the Canada Foundation for Innovation. Y.Z. is also grateful for the financial support from the China Scholarship Council (CSC).

REFERENCES

(1) Kim, K.; Kim, S.; Ryu, J.; Jeon, J.; Jang, S. G.; Kim, H.; Gweon, D.-G.; Im, W. B.; Han, Y.; Kim, H.; Choi, S. Q. Processable High Internal Phase Pickering Emulsions Using Depletion Attraction. *Nat. Commun.* **2017**, *8*, 14305.

(2) Silverstein, M. S. PolyHIPEs: Recent Advances in Emulsion-Templated Porous Polymers. *Prog. Polym. Sci.* **2014**, *39*, 199−234.

(3) Princen, H.; Kiss, A. Rheology of Foams and Highly Concentrated Emulsions: III. Static Shear Modulus. *J. Colloid Interface Sci.* **1986**, *112*, 427−437.

(4) Dickinson, E. Emulsion Gels: The Structuring of Soft Solids with Protein-Stabilized Oil Droplets. *Food Hydrocolloids* **2012**, *28*, 224−241.

(5) Busby, W.; Cameron, N. R.; Jahoda, C. A. Emulsion-Derived Foams (PolyHIPEs) Containing Poly(ε-caprolactone) as Matrixes for Tissue Engineering. *Biomacromolecules* **2001**, *2*, 154−164.

(6) Sommer, M. R.; Alison, L.; Minas, C.; Tervoort, E.; Rühs, P. A.; Studart, A. R. 3D Printing of Concentrated Emulsions into Multiphase Biocompatible Soft Materials. *Soft Matter* **2017**, *13*, 1794−1803.

(7) Wu, D.; Xu, F.; Sun, B.; Fu, R.; He, H.; Matyjaszewski, K. Design and Preparation of Porous Polymers. *Chem. Rev.* **2012**, *112*, 3959−4015.

(8) Bai, L.; Huan, S.; Gu, J.; McClements, D. J. Fabrication of Oil-in-Water Nanoemulsions by Dual-channel Microfluidization Using Natural Emulsifiers: Saponins, Phospholipids, Proteins, and Polysaccharides. *Food Hydrocolloids* **2016**, *61*, 703−711.

(9) Sun, G.; Li, Z.; Ngai, T. Inversion of Particle-Stabilized Emulsions to Form High-Internal-Phase Emulsions. *Angew. Chem., Int. Ed.* **2010**, *49*, 2163−2166.

(10) Viennois, E.; Merlin, D.; Gewirtz, A. T.; Chassaing, B. Dietary Emulsifier-Induced Low-grade Inflammation Promotes Colon Carcinogenesis. *Cancer Res.* **2017**, *77*, 27−40.

(11) Ramsden, W. Separation of Solids in the Surface-Layers of Solutions and 'Suspensions' (Observations on Surface-Membranes, Bubbles, Emulsions, and Mechanical Coagulation).-Preliminary Account. *Proc. R. Soc. London* **1904**, *72*, 156−164.

(12) Pickering, S. U. CXCVI.-Emulsions. *J. Chem. Soc., Trans.* **1907**, *91*, 2001−2021.

(13) Aveyard, R.; Binks, B. P.; Clint, J. H. Emulsions Stabilised Solely by Colloidal Particles. *Adv. Colloid Interface Sci.* **2003**, *100*, 503−546.

(14) Bai, L.; Lv, S.; Xiang, W.; Huan, S.; McClements, D. J.; Rojas, O. J. Oil-in-Water Pickering Emulsions via Microfluidization with Cellulose Nanocrystals: 1. Formation and Stability. *Food Hydrocolloids* **2019**, *96*, 699−708.

(15) Ikem, V. O.; Menner, A.; Bismarck, A. High Internal Phase Emulsions Stabilized Solely by Functionalized Silica Particles. *Angew. Chem., Int. Ed.* **2008**, *47*, 8277−8279.

(16) Sun, C.; Gao, Y.; Zhong, Q. Properties of Ternary Biopolymer Nanocomplexes of Zein, Sodium Caseinate, and Propylene Glycol Alginate and Their Functions of Stabilizing High Internal Phase Pickering Emulsions. *Langmuir* **2018**, *34*, 9215−9227.

(17) Li, Z.; Ming, T.; Wang, J.; Ngai, T. High Internal Phase Emulsions Stabilized Solely by Microgel Particles. *Angew. Chem., Int. Ed.* **2009**, *48*, 8490−8493.

(18) Zhou, F.-Z.; Yu, X.-H.; Zeng, T.; Yin, S.-W.; Tang, C.-H.; Yang, X.-Q. Fabrication and Characterization of Novel Water-Insoluble Protein Porous Materials Derived from Pickering High Internal-Phase Emulsions Stabilized by Gliadin-Chitosan-Complex Particles. *J. Agric. Food Chem.* **2019**, *67*, 3423−3431.

(19) Ikem, V. O.; Menner, A.; Horozov, T. S.; Bismarck, A. Highly Permeable Macroporous Polymers Synthesized From Pickering Medium and High Internal Phase Emulsion Templates. *Adv. Mater.* **2010**, *22*, 3588−3592.

(20) Akartuna, I.; Studart, A. R.; Tervoort, E.; Gauckler, L. J. Macroporous Ceramics From Particle-Stabilized Emulsions. *Adv. Mater.* **2008**, *20*, 4714−4718.

(21) Zhou, S.; Bismarck, A.; Steinke, J. H. Interconnected Macroporous Glycidyl Methacrylate-Grafted Dextran Hydrogels Synthesised From Hydroxyapatite Nanoparticle Stabilised High Internal Phase Emulsion Templates. *J. Mater. Chem.* **2012**, *22*, 18824−18829.

(22) Tan, H.; Sun, G.; Lin, W.; Mu, C.; Ngai, T. Gelatin Particle-Stabilized High Internal Phase Emulsions as Nutraceutical Containers. *ACS Appl. Mater. Interfaces* **2014**, *6*, 13977−13984.

(23) Zeng, T.; Wu, Z.-l.; Zhu, J.-Y.; Yin, S.-W.; Tang, C.-H.; Wu, L.-Y.; Yang, X.-Q. Development of Antioxidant Pickering High Internal Phase Emulsions (HIPEs) Stabilized by Protein/Polysaccharide Hybrid Particles as Potential Alternative for PHOs. *Food Chem.* **2017**, *231*, 122−130.

(24) Gurevitch, I.; Silverstein, M. S. Polymerized Pickering HIPEs: Effects of Synthesis Parameters on Porous Structure. *J. Polym. Sci., Part A: Polym. Chem.* **2010**, *48*, 1516−1525.

(25) Zheng, Z.; Zheng, X.; Wang, H.; Du, Q. Macroporous Graphene Oxide-Polymer Composite Prepared Through Pickering High Internal Phase Emulsions. *ACS Appl. Mater. Interfaces* **2013**, *5*, 7974−7982.

(26) Menner, A.; Ikem, V.; Salgueiro, M.; Shaffer, M. S.; Bismarck, A. High Internal Phase Emulsion Templates Solely Stabilised by Functionalised Titania Nanoparticles. *Chem. Commun.* **2007**, 4274−4276.

(27) Chen, Y.; Ballard, N.; Bon, S. A. Moldable High Internal Phase Emulsion Hydrogel Objects From Non-covalently Crosslinked Poly(N-isopropylacrylamide) Nanogel Dispersions. *Chem. Commun.* **2013**, *49*, 1524−1526.

(28) Bai, L.; Greca, L. G.; Xiang, W.; Lehtonen, J.; Huan, S.; Nugroho, R. W. N.; Tardy, B. L.; Rojas, O. J. Adsorption and Assembly of Cellulosic and Lignin Colloids at Oil/Water Interfaces. *Langmuir* **2019**, *35*, 571−588.

(29) Xu, Y.-T.; Tang, C.-H.; Binks, B. P. High Internal Phase Emulsions Stabilized Solely by a Globular Protein Glycated to Form Soft Particles. *Food Hydrocolloids* **2020**, *98*, 105254.

(30) Xu, Y.-T.; Liu, T.-X.; Tang, C.-H. Novel Pickering High Internal Phase Emulsion Gels Stabilized Solely by Soy β-conglycinin. *Food Hydrocolloids* **2019**, *88*, 21−30.

(31) Xu, Y.-T.; Tang, C.-H.; Liu, T.-X.; Liu, R. Ovalbumin as an Outstanding Pickering Nanostabilizer for High Internal Phase Emulsions. *J. Agric. Food Chem.* **2018**, *66*, 8795−8804.

(32) Xu, Y.-T.; Wang, Y.-H.; Chen, F.-P.; Tang, C.-H. Whether Ovalbumin Performs as A Particulate or Polymeric Emulsifier Is Largely Determined by pH. *Food Hydrocolloids* **2020**, *103*, 105694.

(33) Dai, L.; Yang, S.; Wei, Y.; Sun, C.; McClements, D. J.; Mao, L.; Gao, Y. Development of Stable High Internal Phase Emulsions by Pickering Stabilization: Utilization of Zein-Propylene glycol Alginate-Rhamnolipid Complex Particles as Colloidal Emulsifiers. *Food Chem.* **2019**, *275*, 246−254.

(34) Yan, C.; McClements, D. J.; Zou, L.; Liu, W. A Stable High Internal Phase Emulsion Fabricated with OSA-modified Starch: An Improvement in β-carotene Stability and Bioaccessibility. *Food Funct.* **2019**, *10*, 5446−5460.

(35) Bai, L.; Huan, S.; Xiang, W.; Rojas, O. J. Pickering Emulsions by Combining Cellulose Nanofibrils and Nanocrystals: Phase Behavior and Depletion Stabilization. *Green Chem.* **2018**, *20*, 1571−1582.

(36) Chen, Q.-H.; Zheng, J.; Xu, Y.-T.; Yin, S.-W.; Liu, F.; Tang, C.-H. Surface Modification Improves Fabrication of Pickering High Internal Phase Emulsions Stabilized by Cellulose Nanocrystals. *Food Hydrocolloids* **2018**, *75*, 125−130.

(37) Liu, F.; Zheng, J.; Huang, C.-H.; Tang, C.-H.; Ou, S.-Y. Pickering High Internal Phase Emulsions Stabilized by Protein-Covered Cellulose Nanocrystals. *Food Hydrocolloids* **2018**, *82*, 96−105.

(38) Capron, I.; Cathala, B. Surfactant-Free High Internal Phase Emulsions Stabilized by Cellulose Nanocrystals. *Biomacromolecules* **2013**, *14*, 291−296.

(39) Ling, S.; Chen, W.; Fan, Y.; Zheng, K.; Jin, K.; Yu, H.; Buehler, M. J.; Kaplan, D. L. Biopolymer Nanofibrils: Structure, Modeling, Preparation, and Applications. *Prog. Polym. Sci.* **2018**, *85*, 1−56.

(40) Perrin, E.; Bizot, H.; Cathala, B.; Capron, I. Chitin Nanocrystals for Pickering High Internal Phase Emulsions. *Biomacromolecules* **2014**, *15*, 3766−3771.

(41) Bai, L.; Huan, S.; Xiang, W.; Liu, L.; Yang, Y.; Nugroho, R. W. N.; Fan, Y.; Rojas, O. J. Self-Assembled Networks of Short and Long Chitin Nanoparticles for Oil/Water Interfacial Superstabilization. *ACS Sustainable Chem. Eng.* **2019**, *7*, 6497−6511.

(42) Larbi, F.; García, A.; del Valle, L. J.; Hamou, A.; Puiggalí, J.; Belgacem, N.; Bras, J. Comparison of Nanocrystals and Nanofibers Produced From Shrimp Shell α-chitin: From Energy Production to Material Cytotoxicity and Pickering Emulsion Properties. *Carbohydr. Polym.* **2018**, *196*, 385−397.

(43) Huang, Y.; Yang, J.; Chen, L.; Zhang, L. Chitin Nanofibrils to Stabilize Long-life Pickering Foams and Their Application for Lightweight Porous Materials. *ACS Sustainable Chem. Eng.* **2018**, *6*, 10552−10561.

(44) Fan, Y.; Saito, T.; Isogai, A. Preparation of Chitin Nanofibers From Squid Pen β-chitin by Simple Mechanical Treatment under Acid Conditions. *Biomacromolecules* **2008**, *9*, 1919−1923.

(45) Fan, Y.; Saito, T.; Isogai, A. Individual Chitin Nano-Whiskers Prepared From Partially Deacetylated α-chitin by Fibril Surface Cationization. *Carbohydr. Polym.* **2010**, *79*, 1046−1051.

(46) Liu, L.; Bai, L.; Tripathi, A.; Yu, J.; Wang, Z.; Borghei, M.; Fan, Y.; Rojas, O. J. High Axial Ratio Nanochitins for Ultrastrong and Shape-Recoverable Hydrogels and Cryogels via Ice Templating. *ACS Nano* **2019**, *13*, 2927−2935.

(47) Binks, B. P.; Rodrigues, J. A. Double Inversion of Emulsions by Using Nanoparticles and a Di-chain Surfactant. *Angew. Chem., Int. Ed.* **2007**, *46*, 5389−5392.

(48) Schneider, C. A.; Rasband, W. S.; Eliceiri, K. W. NIH Image to ImageJ: 25 Years of Image Analysis. *Nat. Methods* **2012**, *9*, 671−675.

(49) Al-Sawalmih, A.; Li, C.; Siegel, S.; Fabritius, H.; Yi, S.; Raabe, D.; Fratzl, P.; Paris, O. Microtexture and Chitin/Calcite Orientation Relationship in the Mineralized Exoskeleton of the American Lobster. *Adv. Funct. Mater.* **2008**, *18*, 3307−3314.

(50) Jiao, B.; Shi, A.; Wang, Q.; Binks, B. P. High-Internal-Phase Pickering Emulsions Stabilized Solely by Peanut-Protein-Isolate Microgel Particles with Multiple Potential Applications. *Angew. Chem., Int. Ed.* **2018**, *57*, 9274−9278.

(51) Zafeiri, I.; Horridge, C.; Tripodi, E.; Spyropoulos, F. Emulsions Co-stabilised by Edible Pickering Particles and Surfactants: The Effect of HLB Value. *Colloids Surf., B* **2017**, *100*, 5−9.

(52) Cameron, N.; Sherrington, D. High Internal Phase Emulsions (HIPEs)-Structure, Properties and Use in Polymer Preparation. In *Biopolymers Liquid Crystalline Polymers Phase Emulsion*; Springer: 1996; pp 163−214.

(53) Zhu, Y.; Luo, X.; Wu, X.; Li, W.; Li, B.; Lu, A.; Liu, S. Cellulose Gel Dispersions: Fascinating Green Particles for the Stabilization of Oil/Water Pickering Emulsion. *Cellulose* **2017**, *24*, 207−217.

(54) Liu, S.; Zhu, Y.; Wu, Y.; Lue, A.; Zhang, C. Hydrophobic Modification of Regenerated Cellulose Microparticles with Enhanced Emulsifying Capacity for O/W Pickering Emulsion. *Cellulose* **2019**, *26*, 6215−6228.

(55) Herazo, M. Á.; Ciro-Velásquez, H. J.; Márquez, C. J. Rheological and Thermal Study of Structured Oils: Avocado (Persea americana) and Sacha Inchi (Plukenetia volubilis L.) Systems. *J. Food Sci. Technol.* **2019**, *56*, 321−329.

(56) Palla, C.; Giacomozzi, A.; Genovese, D. B.; Carrín, M. E. Multi-Objective Optimization of High Oleic Sunflower Oil and Monoglycerides Oleogels: Searching for Rheological and Textural Properties Similar to Margarine. *Food Struct.* **2017**, *12*, 1−14.

(57) Primacella, M.; Wang, T.; Acevedo, N. Characterization of Mayonnaise Properties Prepared Using Frozen-Thawed Egg Yolk Treated with Hydrolyzed Egg Yolk Proteins as Anti-Gelator. *Food Hydrocolloids* **2019**, *96*, 529−536.

(58) Liu, L.; Wang, R.; Yu, J.; Jiang, J.; Zheng, K.; Hu, L.; Wang, Z.; Fan, Y. Robust Self-Standing Chitin Nanofiber/Nanowhisker Hydrogels with Designed Surface Charges and Ultralow Mass Content via Gas Phase Coagulation. *Biomacromolecules* **2016**, *17*, 3773−3781.

(59) Huan, S.; Mattos, B. D.; Ajdary, R.; Xiang, W.; Bai, L.; Rojas, O. J. Two-phase Emulgels for Direct Ink Writing of Skin-Bearing Architectures. *Adv. Funct. Mater.* **2019**, *29*, 1902990.

(60) Huan, S.; Ajdary, R.; Bai, L.; Klar, V.; Rojas, O. J. Low Solids Emulsion Gels Based on Nanocellulose for 3D-printing. *Biomacromolecules* **2019**, *20*, 635−644.

(61) Bamba, Y.; Ogawa, Y.; Saito, T.; Berglund, L. A.; Isogai, A. Estimating the Strength of Single Chitin Nanofibrils via Sonication-Induced Fragmentation. *Biomacromolecules* **2017**, *18*, 4405−4410.

(62) Tu, S.; Zhao, Y.; Tan, H.; Yu, H.; Zhu, X.; Wang, H. Ultralight Silica Foams with a Hierarchical Pore Structure via a Surfactant-Free High Internal Phase Emulsion Process. *Langmuir* **2018**, *34*, 10381−10388.